



1  
2  
3  
4  
5  
6  
7  
8  
9  
10  
11  
12  
13  
14  
15  
16  
17  
18  
19  
20  
21  
22  
23  
24  
25  
26  
27  
28  
29  
30  
31  
32  
33  
34  
35

## Are drivers of northern lights in the ionosphere?

Office Geophysik, Ogoori, 838-0141, Japan

Osuke Saka

saka.o@nifty.com

### Abstract

It is reported that transverse electric fields penetrating the ionosphere either from distant space or from the upper atmosphere produce charge separations along the field lines by building up positive charges immediately above the ionosphere. Those parallel electric fields produced by the charge separation deserve auroral driver. This paper discusses why and how these internal drivers in the polar ionosphere are applied for the formation of spiral auroras in the dusk sector.

### 1. Introduction

Known as northern lights, spiral auroras with scale size from 1 km to several hundred km in the polar ionosphere are distinct features of substorms. These auroras are classified as discrete auroras generated by energetic electrons accelerated along the field lines. To explain these spiral patterns, two models are proposed according to rotational direction of the spirals, counterclockwise or clockwise viewed along the field lines. One is a current sheet model of auroras where current sheets originating in the magnetosphere twist along the field lines to show winding auroras at ionospheric altitudes [Hallinan, 1976; Partamies et al., 2001; Keiling et al., 2009]. Spirals are counterclockwise viewed along the field lines in the upward field aligned current region. The second is a charge sheet model where negative charge excess in the ionosphere causes spirals rotating clockwise, opposite to the current sheet model [Hallinan and Davis, 1970; Oguti, 1974]. The second model seems to violate the Gauss's law, because upward electric fields have negative potential regions at their footprint. To resolve this seeming paradox, the ionospheric injection scenario is applied [Saka, 2023].



36 **2. Quasi-neutral equilibrium solutions of the parallel electric fields (steady-state**  
37 **approximation)**

38 Figure 1 shows vertical profiles of electrostatic potential generated above the ionosphere  
39 by the narrow negative charge sheet. The charge sheet is due to local  
40 accumulation/rarefaction of electric charges in the E-layer produced by external electric  
41 fields penetrating the polar ionosphere [Saka, 2021]. The vertical component of electric  
42 fields generated by the negative charge sheet displaced the mirror height of electrons to  
43 higher altitudes, causing a buildup of positive charges immediately above the ionosphere  
44 and negative charges in the magnetosphere [Saka, 2023]. Such charge separations along  
45 the field lines produced parallel electric fields. On the ground, those potential variations in  
46 the ionosphere may be observed as a change of atmospheric electric field in the global  
47 current circuit of the ionosphere-atmosphere-earth system [Tinsley et al., 1998].

48  
49 Parallel electric fields influence temperature anisotropy of particles by changing their pitch-  
50 angle. Disparity in temperature anisotropy between species sustains steady-state parallel  
51 electric fields as quasi-neutral equilibrium solutions [Alfven and Falthammar, 1963;  
52 Persson, 1963, 1966]. For the case of upward electric fields, perpendicular temperature  
53 anisotropy of electrons (  $T_{e\perp} > T_{e\parallel}$  ) exceeds that of ions at any point of B. Upward electric  
54 fields thus produced by a narrow negative charge sheet constitute 1-D inverted-V above  
55 the ionosphere (Figure 2). Generation of upward electric fields above the negative charge  
56 sheet is analogous to a battery connected in series to a negative electrode in the  
57 ionosphere.

58  
59 The parallel electric fields may persist until charge separation along field lines is discharged  
60 due to reduction of perpendicular temperature anisotropy of electrons by pitch-angle  
61 diffusion of electrons [Kennel and Petschek, 1966]. Discharge may occur locally and  
62 intermittently accompanying auroral precipitation. Such correlations are reported in the  
63 paper titled "Hiss emitting auroral activity" [Oguti, 1975a]. Flux tube filling perpendicular  
64 temperature anisotropy of electrons corresponds to area in polar ionosphere having higher  
65 occurrence probability of aurora. Those areas are a part of auroral oval. If expansion  
66 speeds of the discharge in the flux tube remain much the same after onset, the lifetime of  
67 the spiral auroras is linearly proportional to the scale size of the flux tube, shorter for  
68 smaller size and longer for larger size. According to Oguti (1975b), expansion speeds  
69 range in 6-8 km/s independent of their scale size from 1 km to 1000 km. Parallel electric  
70 fields vanish when perpendicular temperature anisotropy of electrons become equal to that  
71 of ions at any point of B.



72

73

### 74 3. Clockwise spirals

75 We apply this ionospheric driver scenario to explain typical spiral auroras winding clockwise  
76 in the dusk sector. Those are known as “S-shaped structure” [Oguti, 1975b]. First, we  
77 assume precipitating electrons due to a discharge produced narrow sheet (1-D) of ion  
78 holes at the footprint of inverted-V potential. Because longitudinal extent of the ion hole is  
79 limited, electric fields converging in the center of the sheet develop along the sheet. Figure  
80 3 depicts amplitude profiles of electrostatic potential ( $\Phi$ ), electric fields ( $E$ ), and density  
81 difference between ions and electrons ( $n_i - n_e$ ) in the ion hole.  $X$  denotes a distance from  
82 the center of the hole. Amplitudes of  $\Phi$ ,  $E$ ,  $n_i - n_e$ , and distance  $X$  are in arbitrary scale.  
83 The ion hole ( $-40 < X < 40$ ) is composed of electron rich regions ( $n_e > n_i$ ) in  $-27 < X < 27$   
84 and ion walls ( $n_i > n_e$ ) peaked at  $X = -37, 37$ . Total charges of ions and electrons are  
85 balanced. The profile of the density difference ( $n_i - n_e$ ) is integrated with  $X$  to calculate  
86 electric fields and electrostatic potentials. It is assumed that this potential structure was  
87 retained for some time ( $\sim 1$  min), because ion holes are continuously produced by the  
88 discharge.

89

90 A winding motion of auroral sheet is caused by the space charge fields in the ion hole  
91 through ExB drift. The sequence of activities is believed to include: (1) exit motion of  
92 inverted-V potentials followed drift motion of auroral sheet, (2) one dimensional potential  
93 profile of ion hole in Figure 3 is conserved during the winding motion, and (3) ion rich  
94 region appears at the edge of the ion hole to maintain charge balance. The results are  
95 shown in Figure 4 in which auroral sheet rotated clockwise around the center viewed in a  
96 direction parallel to the background field lines. Auroral sheet developed expanding in length  
97 during rotation and left folding pattern at the center. Clockwise motions at the center  
98 reproduce “Curls” of charge sheet [Hallinan and Davis, 1970] or “Trailing rotation” [Figure  
99 2b in Oguti, 1974]. A clockwise flapping motion of narrow auroral sheet may correspond to  
100 the “Flame-structure formation” in a rotation of the flame trains [Figure 5 in Oguti, 1975b],  
101 “Clockwise turning-over” in the process of poleward expansion of aurora [Figure 2 in Oguti,  
102 1981], and “Splitting-fold over deformation” of a discrete arc in small-scale [Figure 3 in  
103 Oguti, 1981]. Figure 5 depicts twist motion of the auroral sheet in a background arc. The  
104 rotating arc in the background yields characteristic deformations referred to as “Splitting  
105 followed by rotational unfolding” of a discrete arc [Figure 1 in Oguti, 1978].



106

107

108 **4. Summary and discussion**

109 Because of rotational symmetry deformation of small- and large-scale S-shaped spirals at a  
110 constant speed (6–8 km/s), it has been suggested that common physical processes may  
111 explain the deforming processes involved [Oguti, 1975b]. The internal processes of the  
112 polar ionosphere referred to as ionospheric injection partly correspond to common physical  
113 processes.

114

115 Required conditions for this ionospheric driver scenario generating substorm auroras are  
116 the ionosphere itself as well as transverse electric fields, originating either from distant  
117 space (field line dipolarization) or from the upper atmosphere (neutral winds). The  
118 ionospheric driver scenario proposed can accordingly be applied to any planets in the Solar  
119 system.

120

121 It is shown that auroral deformations starting with a splitting of the auroral arc that are  
122 referred to as S-shaped structures can be adequately explained by the ionospheric driver  
123 scenario. However, an ionospheric driver scenario may not be equally applicable to spiral  
124 auroras starting with a folding of the auroral arc (current sheet model). In that case, a  
125 magnetospheric driver scenario may be appropriate. Developed spiral forms are identical in  
126 both scenarios. To distinguish between the two scenarios in substorm auroras, deformation  
127 processes should be carefully examined to determine whether spiral auroras start with a  
128 folding of the auroral arc or a splitting of the auroral arc (Figure 6).

129

130

131 **5. Data availability**

132 No data sets were used in this article.

133

134

135 **6. Competing interest**

136 The author declares that there is no conflict of interest.

137

138

139

140

141



- 142  
143  
144 Alfven, H. and Falthammar, C.-G.: *Cosmical Electrodynamics*, 2<sup>nd</sup> Edn., Oxford University  
145 Press, New York, 1963.  
146 Hallinan, T.J.: Auroral spirals 2. Theory, *J. Geophys. Res.*, **81**, 3959-3965, 1976.  
147 Hallinan, T.J., & Davis, T.N.: Small-scale auroral arc distortions. *Planet Space Sci.*, **18**,  
148 1735-1744, 1970.  
149 Keiling, A., Angelopoulos, V., Weygand, J.M., Amm, O., Spanswick, E., Donovan, E.,  
150 Mende, S. McFadden, J., Larson, D., Glassmeier, K.-H., and Auster H.U.: THEMIS  
151 ground-space observations during the development of auroral spirals, *Ann. Geophys.*,  
152 27, 4317-432, 2009.  
153 Kennel, C.F., and Petschek, H.E.: Limit of stably trapped particle fluxes, *J. Geophys. Res.*,  
154 71, 1-28, 1966.  
155 Oguti, T.: Rotational deformations and related drift motions of auroral arcs, *J. Geophys.*  
156 *Res.*, 79, 3861-3865, 1974.  
157 Oguti, T.: Hiss emitting auroral activity, *J. Atmos. Terr. Phys.*, 37, 761-768, 1975a.  
158 Oguti, T., Similarity between global auroral deformations in DAPP photographs and small  
159 scale deformations observed by a TV camera, *J. Atmos. Terr. Phys.*, **37**, 1413-1418,  
160 1975b.  
161 Oguti, T.: Observations of rapid auroral fluctuations, *J. Geomag. Geoelectr.*, **30**, 299-314,  
162 1978.  
163 Oguti, T.: TV observations of auroral arcs, *AGU Geophysical Monograph Series*, Vol 25  
164 (Physics of auroral arc formation), 31-41, 1981.  
165 Partamies, N., Freeman, M.P., and Kauristie, K.: On the winding of auroral spirals:  
166 Interhemispheric observations and Hallinan's theory revisited, *J. Geophys. Res.*, 106,  
167 28913-28924, 2001.  
168 Persson, H.: Electric field along a magnetic line of force in a low-density plasma, *Physics*  
169 *Fluids*, 6, 1756-1759, 1963.  
170 Persson, H.: Electric field parallel to the magnetic field in a low-density plasma, *Physics*  
171 *Fluids*, 9, 1090-1098, 1966.  
172 Saka, O.: Ionospheric control of space weather, *Ann. Geophys.*, 39, 455-460, 2021.  
173 Saka, O.: Parallel electric fields produced by ionospheric injection, *Ann. Geophys.*, 41, 369-  
174 373, 2023.  
175 Tinsley, B.A., Liu, W., Rohrbaugh, R.P., and Kirkland, M.W.: South Pole electric field  
176 responses to overhead ionospheric convection, *J. Geophys. Res.*, 103, 26137-26146,  
177 1998.



178

179

180

181

182

#### Figure captions

183

184 Figure 1

185 Electrostatic potentials produced in vertical planes (X-Y, Z=0) and (X-Z, Y=0) by negative  
186 charge sheet in the ionosphere (Y-Z plane). Scales are arbitrary. Potential increases  
187 radially outward from the center of the sheet or with altitudes (X). The sheet is narrow in Z,  
188 10% of Y. Green bars denote extent of negative charge sheet in Y (upper panel) and in Z  
189 (lower panel). Vertical component of the electric fields produces positive charge  
190 immediately above the ionosphere.

191

192 Figure 2

193 Inverted-V (battery) connected in series directly to the ionosphere (negative electrode).  
194 Ionospheric potential beneath the inverted-V is assumed to be negative, and 0 volt in the  
195 surroundings. Inverted-V potential is consisted of steady-state parallel electric fields.  
196 Auroral precipitations are due to discharge of the steady-state parallel electric fields,  
197 occurring locally and intermittently in the inverted-V. Precipitations create ion holes in the  
198 ionosphere (see Figure 3).

199

200 Figure 3

201 One dimensional ion hole in X represents auroral sheet. The ion hole model is applied to  
202 the auroral sheets independent of their scale size. Electric field profile marked by dotted  
203 arrow is used in Figure 4 to show a twist motion of the auroral sheet.

204

205 Figure 4

206 Clockwise rotation of auroral sheet. The auroral sheet initially in the east-west directions in  
207 black (T=0) deformed to red (T=Δt), green (T=2Δt), blue (T=3Δt), and to purple (T=4Δt) in  
208 X-Y plane. X is east and Y is north. These motions were caused by the space charge fields  
209 in the ion hole through  $E_{\perp} \times B$  drift.

210

211 Figure 5

212 Rotating motion of auroral sheet in background arc. Auroral sheet is marked in Black in the  
213 pre-existing background auroral arc (Light Cyan). Auroras are void in the white area



214 removed by the rotating exit. Background arc was split while the exit rotated clockwise from  
215 (A) to (B). Unfolding deformation follows (C) through (E) and is finally released in (F), and  
216 (G). Sequence of the auroral sheet deformations from split of background arc, pleat  
217 unfolding, and its release referred to as “Splitting-unfolding deformation of auroral pleat”  
218 are illustrated in the right-bottom corner [adapted from Oguti, 1975b].

219

220 Figure 6

221 (A) Deformation of spiral auroras starting with splitting of auroral sheet. (B) Deformation of  
222 spiral auroras starting with folding. Initial auroral forms associated with splitting and folding  
223 are shown in red. In (A), auroral sheet twists clockwise viewed in a direction parallel to the  
224 field lines. In (B), auroral sheet rotates counterclockwise. Developed auroral sheets in blue  
225 are identical for (A) and (B).

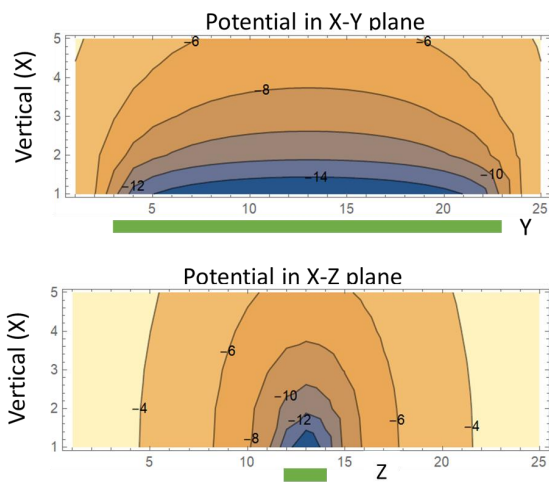
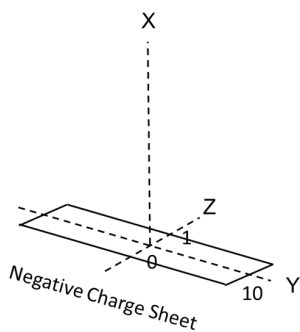


Figure 1

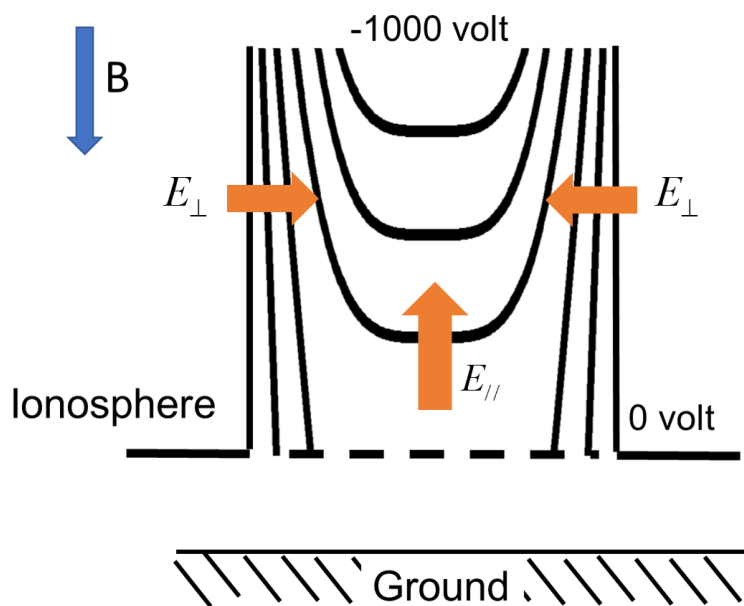


Figure 2

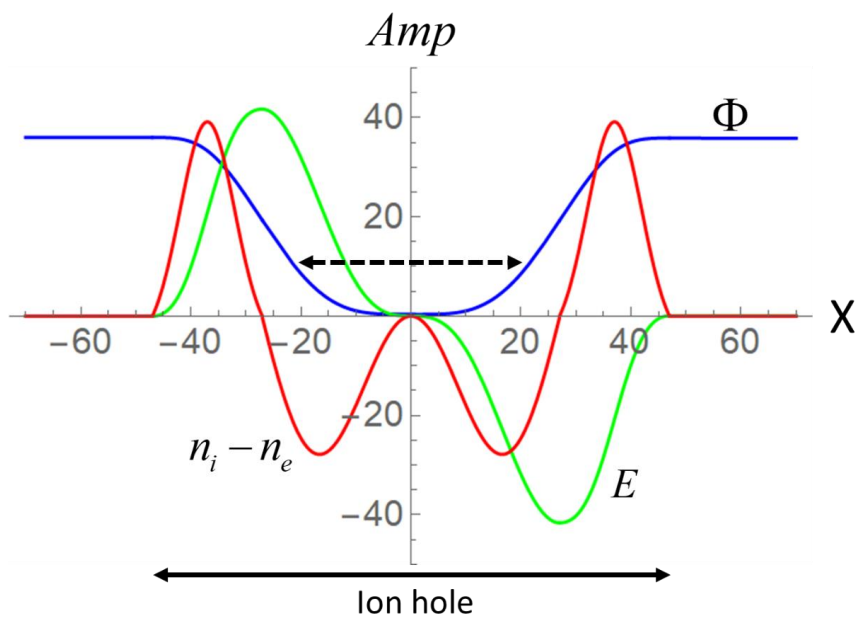


Figure 3

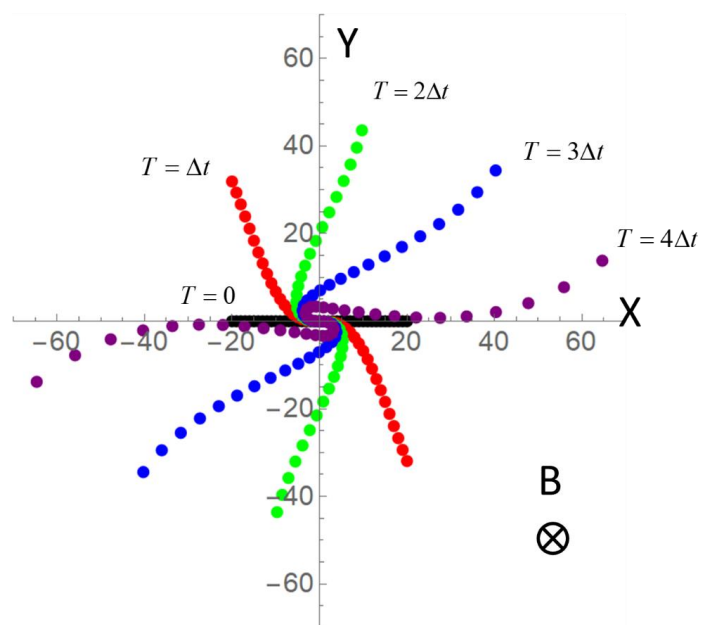


Figure 4

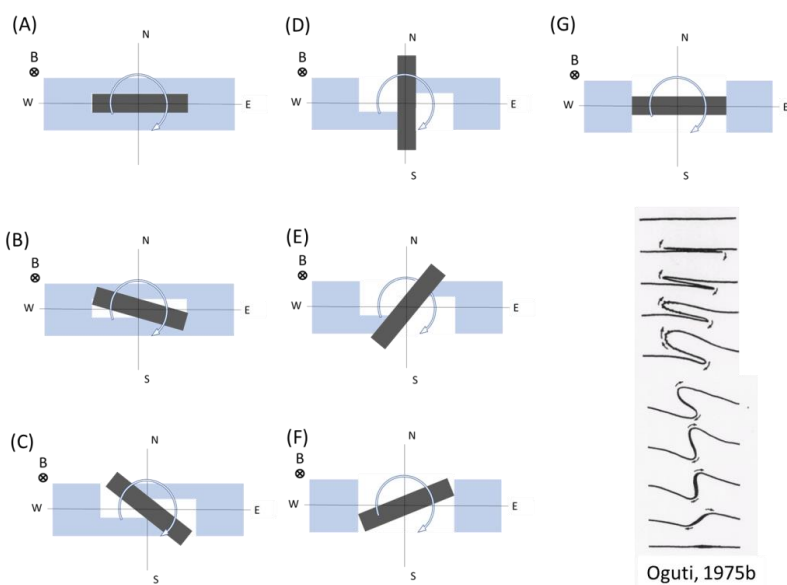


Figure 5

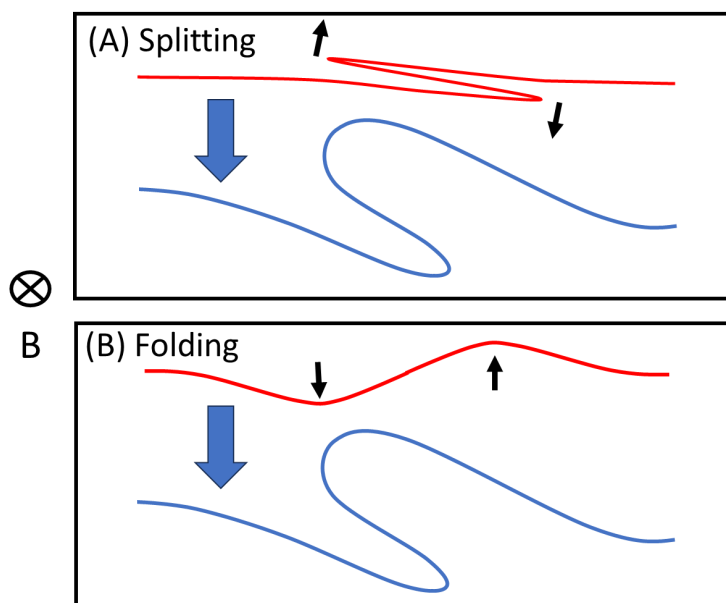


Figure 6